Soluble Guanylate Cyclase Reduced the Gastrointestinal Fibrosis in Bleomycin-induced Mouse Model of Systemic Sclerosis.

Yuzuru Yamamoto
Kobe University Graduate School of Medicine School of Medicine: Kobe Daigaku Daigakuin Igakukei Kenkyuka Igakubu

Takaichi Okano
Kobe University Graduate School of Medicine School of Medicine: Kobe Daigaku Daigakuin Igakukei Kenkyuka Igakubu

Hirotaka Yamada
Kobe University Graduate School of Medicine School of Medicine: Kobe Daigaku Daigakuin Igakukei Kenkyuka Igakubu

Kengo Akashi
Kobe University Graduate School of Medicine School of Medicine: Kobe Daigaku Daigakuin Igakukei Kenkyuka Igakubu

Sho Sendo
Kobe University Graduate School of Medicine School of Medicine: Kobe Daigaku Daigakuin Igakukei Kenkyuka Igakubu

Yo Ueda
Kobe University Graduate School of Medicine School of Medicine: Kobe Daigaku Daigakuin Igakukei Kenkyuka Igakubu

Akio Morinobu
Kobe University Graduate School of Medicine School of Medicine: Kobe Daigaku Daigakuin Igakukei Kenkyuka Igakubu

Jun Saegusa (jsaegusa@med.kobe-u.ac.jp)
Kobe University Graduate School of Medicine School of Medicine: Kobe Daigaku Daigakuin Igakukei Kenkyuka Igakubu

---

Research article

Keywords: Systemic sclerosis, gastrointestinal fibrosis, soluble guanylate cyclase

Posted Date: January 5th, 2021

DOI: https://doi.org/10.21203/rs.3.rs-138442/v1

Abstract

Background: Systemic sclerosis (SSc) is a chronic autoimmune-mediated connective tissue disorder. Although the etiology of the disease remains undermined, SSc is characterized by fibrosis and proliferative vascular lesions of the skin and internal organs. SSc involves the gastrointestinal tract in more than 90% of patients. Soluble guanylate cyclase (sGC) is used to treat pulmonary artery hypertension (PAH), and has been shown to inhibit experimental skin fibrosis.

Methods: Female C57BL/6J mice were treated with BLM or normal saline by subcutaneous implantation of osmotic minipump. These mice were sacrificed on day 28 or day 42. Gastrointestinal pathologies were examined by Masson Trichrome staining. The expression of fibrosis-related genes in gastrointestinal tract were analyzed by real-time PCR, and the levels of collagen in the tissue was measured by Sircol collagen assay. To evaluate peristaltic movement, the small intestinal transport (ITR%) was calculated as [Dyeing distance×(Duodenum- Appendix)] -1 ×100 (%). We treated BLM-treated mice with soluble guanylate cyclase (sGC) or DMSO orally and analyzed them on day 42.

Results: Histological examination revealed that fibrosis from lamina propria to muscularis mucosa in the esophagus was significantly increased in BLM-treated mice, suggesting that BLM induces esophageal fibrosis in C57BL/6J mice. In addition, the levels of Col3a1 and CTGF were significantly increased in BLM-treated mice. More severe fibrosis was observed in the mice sacrificed on day 42 than the mice sacrificed on day 28. The ITR% was found to be significantly lower in BLM-treated mice, suggesting that gastrointestinal peristaltic movement was reduced in BLM-treated mice. Furthermore, we demonstrated that sGC treatment significantly reduced fibrosis of esophagus and intestine in BLM-treated mice, by histological examination and Sircol collagen assay.

Conclusions: These findings suggest that BLM induces gastrointestinal fibrosis in C57BL/6J mice, and treatment with sGC improves the BLM-induced gastrointestinal lesion.

Background

Systemic sclerosis (SSc) is a connective-tissue disease of unknown etiology. SSc is characterized by autoimmunity, microvascular impairment, chronic inflammation, and fibrotic changes in various organs [1]. There are several mouse models of SSc which develop dermal thickening and fibrosis, the most obvious feature of human SSc. However, they exhibit only some aspects of the disease or develop additional abnormalities not associated with SSc in humans [2].

Bleomycin (BLM) is a chemotherapeutic agent that is used in the management of some human malignancies such as lymphomas and squamous cell carcinomas. The major limitation of BLM therapy is pulmonary toxicity and skin fibrosis [3]. On the other hand, BLM-treated mice are widely accepted as an experimental model of SSc and are mainly used for estimating skin fibrosis. Lee et al. recently reported that systemic delivery of BLM using osmotic minipumps caused lung fibrosis from a peripheral lung lesion, which is similar to the lung fibrosis observed in human SSc patients [4].

On the other hand, more than 90% of SSc patients develop gastrointestinal tract fibrosis. The fibrosis extends from the mouth to the anus, and the esophagus and anorectum are most frequently affected [5] [6]. The esophageal fibrosis causes a reduced quality of life in SSc patients due to gastroesophageal reflux disease and decreased peristaltic movement. Nevertheless, only symptomatic treatment is currently available for gastrointestinal manifestations in SSc [6]. In addition, there have been few reports of mouse models that reproduce the gastrointestinal lesions of SSc. [5] [7]. An epithelial Fli1-deficient mouse has been reported to develop skin, lung, and esophagus fibrosis [8]. The transgenic mouse strain TβRIIδk-fib is characterized by ligand-dependent up-regulation of TGFβ signaling and has been shown to develop skin and lung fibrosis. This TG mouse model was previously shown to develop colonic fibrosis [9]. However, there have been no reports about gastrointestinal fibrosis in BLM-treated mice.

A soluble guanylate cyclase (sGC) stimulator is known as a drug for treatment of pulmonary arterial hypertension in SSc patients. This treatment stimulates soluble guanylate cyclase, increasing cyclic guanosine monophosphate (cGMP) levels and activating protein kinase G (PKG) in the cytosol, resulting in subsequent relaxation of vascular smooth muscle cells. In addition, recent studies have shown that sGC dose-dependently inhibits the fibrosis of kidney, skin, liver, and intestine in several mouse models, thus playing a critical role in fibrotic disease [10]. For example, sGC reduces skin and intestinal fibrosis in experimental sclerodermatous chronic graft-versus-host-disease (Scl-GvHD) [11].

In this study, we provide the first demonstration that continuous subcutaneous administration of BLM induced gastrointestinal fibrosis in mice, which histologically resembled human SSc. In addition, peristaltic movement was significantly impaired in the mice. Furthermore, we revealed that treatment with an sGC agonist ameliorated gastrointestinal fibrosis in the esophagus and intestine of BLM-treated mice.

Materials And Methods

Animals.

Female C57BL/6 mice aged 8 to 9 weeks old were obtained from CLEA Japan, Inc. (Osaka, Japan). We used the mice from 9 to 10 weeks of age. These mice were housed in the animal facility of Kobe University, with a 12-h dark/light cycle at a constant temperature and were provided with food and water *ad libitum*. All procedures were carried out in accordance with the recommendations of the Institutional Animal Care Committee of Kobe University.

Reagents.

BLM was purchased from Nippon Kayaku (Tokyo, Japan). Dimethyl sulfoxide (DMSO) and 2 M acetic acid were purchased from Sigma–Aldrich (St. Louis, MO, USA). A soluble guanylate cyclase stimulator (BAY 63-2521) was purchased from Selleck Chemicals (Houston, TX, USA). Sircol collagen assay was purchased from Biocolor Ltd. (Belfast, UK). Alzet mini-osmotic pumps model 2001 were purchased from Durect Corporation (Cupertino, CA, USA). Disposable oral tubes (disposable feeding needle FG5202) were

purchased from Fuchigami Corporation (Kyoto, Japan). RNeasy Mini kits were purchased from Qiagen (Tokyo, Japan).

BLM administration.

BLM was dissolved in normal saline (NS). BLM or NS were administered with osmotic minipumps, as described in previous reports, with minor modifications [4] [12] [13]. The osmotic minipumps containing 200 μL of BLM (125 mg/kg) or NS were implanted subcutaneously under the loose skin on the backs of C57BL/6 mice on day 0. The pumps delivered 1.0 mg/h for 7 days. The mice were euthanized on day 28 (4 w) or on day 42 (6 w).

For the sGC treatment experiment, we removed these pumps on day 7, then administered 200 μL daily DMSO or sGC orally to mice from day 14 to day 42.

The mice were sacrificed on day 42 (6 w) and gastrointestinal lesions were harvested.

Histology and immunohistochemistry.

The esophageal and intestinal samples were fixed in 4% paraformaldehyde, embedded in paraffin, sectioned, and stained with Masson's trichrome (MT). To evaluate the esophageal and intestinal fibrosis caused by BLM treatment, we measured the thickness between the top of the fibrosis layer and the muscularis mucosa at 40 × magnification under a BZ-X700 fluorescence microscope (Keyence, Osaka, Japan). We analyzed the full length of the esophagus and the intestine up to 5 cm from the pylorus.

Changes in body weight.

We evaluated the change in body weight of the mice from day 0 to day 28 or day 42. The change was calculated using the following formula:

Body weight change (%) = [(body weight on day 28 or on day 42) - (body weight on day 0)] × 1/ (body weight on day 0) × 100 (%).

Gastrointestinal transit.

We examined the small intestinal transport rate (ITR%) as an indicator of gastrointestinal movement [14]. First, the mice were fasted overnight but given free access to water. Two hundred microliters of Evans blue solution (5% w/v in NS) was then orally administered to each mouse and dye distance was evaluated. All animals were sacrificed 30 min after Evans blue solution administration, and the rate of gastrointestinal transit was calculated by dividing the distance of the Evans blue migration by the total length of the small intestine. Specifically, the full length of intestine from the pylorus to the ileocecum and the length between the pylorus and the forefront of the transported dye (distance of dye movement) were measured. The ITR% was calculated using the following formula.

Small intestinal transport rate (%) (ITR%) = [distance of dye movement (cm) / total length of small intestine (cm)] × 100.

Quantitative real-time polymerase chain reaction (rt-PCR).

We examined gene expression in the esophagus and intestine by qPCR to indicate fibrotic gene expression. Total RNA was isolated from the esophagus and intestine using an RNeasy Mini kit purchased from Qiagen, and complementary DNA was reverse-transcribed using a QuantiTect Reverse Transcription kit (Qiagen). PCR reaction mixtures were prepared using the QuantiTect SYBR Green PCR kit (Qiagen). The results were indicated on a PikoReal system. The following primer pairs were used: glyceraldehyde-3-phosphate dehydrogenase (GAPDH), 5'-AACTTTGGCATTGTGGAAG-3' (forward) and 5'-ACACATTGGGGGTAGGAACA-3' (reverse); collagen 3a1 (COL3A1), 5'-CAAGGTCTTCCTGGTCAGCCT-3' (forward) and 5'-TGCCACCAGGAGGAGATCCATCTC-3' (reverse); collagen tissue growth factor (CTGF), 5'-CACTCCGGGAAATGCTCCATGTTG-3' (forward) and 5'-GTTGGGTCTGGGCCAAATGT-3' (reverse); interleukin-6 (IL-6), 5'TTCCATCCAGTTGCCTTCTTG-3' (forward) and 5'-TCATTTCCACGATTTCCCAGAG-3' (reverse); smooth muscle actin (αSMA), 5'-AGAGACTCTCTTCCAGCCATC-3' (forward) and 5'-ACACATTGGGGGTAGGAACA-3' (reverse); collagen 1a1 (COL1A1), 5'-TGACTGGAAGAGCGGAGAGTACT-3' (forward) and 5'-GGTCTGACCTGTCTCCATGTTG-3' (reverse). GAPDH was used as the internal control to normalize the amount of loaded, complementary DNA (cDNA).

Measurement of soluble collagen content.

Sircol collagen assay (Biocolor Ltd, Belfast, UK) was used to quantify soluble collagen content of the esophagus and intestine. Briefly, we measured the weight of the esophagus and intestine, then homogenized each tissue. We mixed the homogenate with 100 mL of acid-neutralizing reagent, and 200 mL of cold isolation & concentration reagent, then added 1 mL of Sircol dye reagent, mixed and allowed to stand for 30 minutes. After centrifugation, the pellets were dissolved in 750 mL of ice-cold acid salt wash regent and 250 mL of Sircol alkali reagent and vortexed. Relative absorbance was measured at 540 nm.

Statistical analysis.

Data are presented as mean ± standard error of the mean (SEM). Differences between groups were analyzed by unpaired t test with Welch's correction, one way ANOVA and Tukey's multiple comparison test using GraphPad Prism 5 software (GraphPad Software Inc., La Jolla, CA, USA).

Results

BLM caused esophageal and intestinal fibrosis.

We first evaluated whether BLM induced gastrointestinal fibrosis in female C57BL/6J mice. We administered BLM (125 mg/kg) or NS by subcutaneous implantation of an osmotic mini-pump on day 0,

and sacrificed the mice on day 28 (4 w) or day 42 (6 w) (Fig. 1A). BLM-treated mice exhibited decreased body weight (Fig. 1B), but no mice died as a result of the implantation itself or the drug administration. We found that BLM treatment increased the distance from the top of the lamina propria to the muscularis mucosa in the esophagus and small intestine (Fig. 1C–F). These results confirmed that BLM-treated mice had significantly increased esophageal and intestinal fibrosis compared with NS-treated mice. Additionally, we showed that more severe esophageal fibrosis was observed in the mice sacrificed at 6 w compared to those sacrificed at 4 w. Also, we confirmed that BLM treatment caused lung and skin fibrosis in mice as previously reported (data not shown).

BLM induced fibrotic gene expression in murine esophagus.

Next, we evaluated fibrotic gene expression in murine esophagus and intestine. The gene expression levels of COL3A1, CTGF and IL-6 in esophagus were significantly increased in BLM-treated mice compared with NS-treated mice (Fig. 2). These results indicated that BLM treatment caused esophageal fibrosis, as reflected in gene expression levels.

We also evaluated gene expression levels of the intestine. There was no significant difference in the expression levels of fibrotic genes between BLM-treated mice and NS-treated mice, although their expression levels tended to be higher in BLM-treated mice than in NS-treated mice (Additional file 1; Additional Fig. 1).

BLM treatment reduced the peristaltic distance of the upper gastrointestinal tract.

Most SSc patients have decreased peristaltic movement of the intestine, leading to chronic intestinal pseudo obstruction (CIPO). Consequently, we next investigated the effect of BLM on peristaltic movement in mice. We analyzed the ITR% to evaluate peristalsis in the upper gastrointestinal tract (Fig. 3A). The ITR% of mice treated with BLM for 6 w was significantly reduced compared to that of NS-treated mice (**$P < 0.01$) (Fig. 3B). This result suggested that BLM-induced gastrointestinal fibrosis impaired peristaltic movement of gastrointestinal involvement. Our results showed that BLM caused gastrointestinal fibrosis both histologically and functionally, resembling the gastrointestinal lesions of SSc patients.

sGC treatment improved esophageal and intestinal fibrosis.

We next examined the effect of methyl (4, 6-diamino-2-(1-(2-fluorobenzyl)-1H-pyrazolo[3, 4-b] pyridine-3-yl) pyrimidin-5-yl) (methyl) carbamate; Riociguat, BAY 63-2521, a stimulator of sGC, which is a drug used to treat pulmonary arterial hypertension in SSc patients. We administered DMSO or BAY 63-2521 orally to BLM-treated mice. The study design of the sGC-stimulation experiment is described in Fig. 4A. No mice died as a result of the experimental procedures. BLM treatment caused a decrease in body weight, while BAY 63-2521 had no effect (Fig. 4B). We found that histological fibrosis was significantly reduced in the esophagus of BAY 63-2521-treated mice compared to DMSO-treated mice (Fig. 4C, 4E). We next measured soluble collagen content of the esophagus and intestine by Sircol collagen assay. BLM significantly increased the soluble collagen content of the esophagus, and BAY 63-2521 significantly

decreased the soluble collagen content induced by BLM (Fig. 4G). In addition, we confirmed that BAY 63-2521 treatment decreased the thickness from the top of the lamina propria to the muscularis mucosa and the soluble collagen content in the intestine of BLM-treated mice (Fig. 4D, 4F, 4H). These results demonstrated that oral sGC-stimulation therapy ameliorated the gastrointestinal fibrosis induced by BLM.

Discussion

In this study, we provided the first evidence that BLM caused gastrointestinal fibrosis, demonstrated both histologically and functionally. The gastrointestinal lesions of SSc patients included esophageal dysmotility, lower esophageal sphincter insufficiency, gastroesophageal reflux, esophageal stricture, a reduction in motility in the intestine, wide-mouthed diverticula in the large intestine and rectal atonia in advanced cases [15]. BLM-induced gastrointestinal lesions resembled several patterns of gastrointestinal lesions observed in SSc patients. In particular, we found that esophageal fibrosis induced by BLM in mice were similar to the esophageal lesions of SSc patients in terms of increasing thickness of the muscularis mucosa observed by MT staining.

BLM causes inflammation by activating the TGFβ and p53 pathways. These activations result in proliferation of fibroblasts and induce apoptosis of epithelial cells, which in turn cause fibrosis. Previously, BLM has been reported to cause intestinal inflammation by increasing tumor necrosis factor α (TNFα), lipopolysaccharide (LPS), and IL-1β [16]. In our experiments, the gene expression level of IL-6 in the esophagus of BLM-treated mice was significantly increased compared with those of NS-treated mice. This inflammation is a pre-requisite for the initiation of fibrotic lesions [17].

In this mouse model, BLM administration caused an increase in the thickness of gastrointestinal fibrosis and reduced peristaltic distance. The gene expression levels of COL3A1 and CTGF in the esophagus of BLM-treated mice were significantly increased compared with those of NS-treated mice. Mishra et al. previously reported that esophageal fibrosis affected the area from the lamina propria to the muscularis mucosa of trichrome-stained paraffin-embedded esophagus in mice and human [18]. Therefore, we measured the fibrotic thickening between the top of the lamina propria and the muscularis mucosa after histopathological staining. Additionally, colon fibrosis is an important part of gastrointestinal fibrosis. A dreaded complication in individuals with SSc is CIPO, which is characterized by bowel dilatation and abnormal motility, and colon fibrosis is an important cause of chronic intestinal failure in patients with SSc [19]. Although fibrosis in the colon is an important feature of gastrointestinal lesions in humans with SSc, we found no evidence of colon fibrosis in this mouse model (data not shown).

The mice treated with BLM for 4 weeks exhibited significantly different patterns of esophageal fibrosis compared to those treated for 6 weeks. However, the severity of inflammation during the onset of fibrogenesis did not correlate with collagen deposition in the mouse model of intestinal fibrosis [17]. Lee et al. previously reported that the lung fibrosis induced by BLM spontaneously decreased after more than 6 weeks [4]. We considered that the period after inflammation might be particularly important. For these

reasons, we decided to sacrifice the mice at 6 weeks after BLM administration; however, this might not have been enough time to observe colon fibrosis.

In previous reports, animal models of intestinal fibrosis were classified into seven categories: spontaneous, gene-targeted, chemical-, immune-, bacteria-, and radiation-induced as well as postoperative fibrosis [20]. However, we were unable to find a suitable mouse model for human SSc which caused fibrosis in the esophagus and intestine simultaneously after chronic inflammation. For example, the dextran sodium sulfate (DSS) -induced intestinal fibrosis model mouse is the easiest and the most reproducible protocol to induce colonic inflammation with associated fibrosis. However, in this mouse model, fibrosis is induced after acute chemical injury and no esophageal lesion has been documented [20]. Another model, the TGFβ1-overexpression mouse, develops colonic fibrosis with obstruction. However, the intestinal fibrosis of this mouse is focal [20]. There have not been any reports of a mouse model in which esophageal and intestinal fibrosis are caused simultaneously. In our mouse model, it is significant that the esophagus and the intestine both exhibit fibrotic changes at the same time.

sGC induces production of cGMP and PKG, which cause vasorelaxation in vascular smooth muscle cells. The *de novo* synthesis of collagen type I is reduced by sGC due to the inhibition of TGFβ-induced ERK1/2 signaling in human lung fibroblasts [21]. In previous reports, treatment with the sGC agonist Riociguat, improved the histological fibrosis and hydroxyproline content in intestine compared with control in Scl-GVHD mice. TGFβ plays a central role in fibrosis in Scl-GVHD mice [11] [22]. We demonstrated that BLM induced gastrointestinal fibrosis in mice. TGFβ1 is known to be involved in BLM-induced organ fibrosis, and activation of TGFβ1 causes fibroblast proliferation [23]. There are several common mechanisms by which cGMP elevation can elicit anti-fibrotic effects. First, cGMP elevation inhibits TGFβ-induced ECM production. Second, cGMP elevation inhibits TGFβ-induced fibroblast to myofibroblast differentiation. Third, cGMP elevation inhibits TGFβ-induced cell proliferation. [10] [24]. As sGC stimulation inhibited gastrointestinal fibrosis in our BLM-treated mice, TGFβ1 may also be involved in BLM-induced gastrointestinal lesions. In our experiments, the gene expression levels of TGFβ1 in the esophagus of BLM-treated mice were significantly increased compared with those of NS-treated mice. Also, the gene expression levels of TGFβ in the esophagus of sGC-stimulation treated mice tended to be lower than those of BLM-treated mice (data not shown).

On the other hand, Hemnes et al. recently reported that PKG activity was decreased by BLM exposure in the lung [25]. sGC stimulation might increase PKG activation in lesions exposed to BLM, which may have been responsible for the therapeutic effect. However, we do not consider that sGC stimulation alone provided the perfect treatment. In fact, sGC stimulation did not significantly improve ITR% (data not shown). These may have been affected by the duration of sGC stimulant treatment.

Riociguat (BAY 63-2521) is known to improve pulmonary arterial hypertension associated with connective tissue diseases (PATENT-1 and PATENT-2) [26]. However, it remains unknown whether Riociguat improves organ fibrosis in SSc. In the RISE-SSc trial and a pilot study, Riociguat did not show a significant effect on the cutaneous lesions of SSc [27] [28]. There has been no report of the effect of Riociguat on

gastrointestinal involvement of SSc patients partly because intestinal lesions are difficult to evaluate. Our mouse model may be a simple and usable model to study the gastrointestinal lesions of SSc.

Conclusion

This study demonstrated that BLM induced gastrointestinal fibrosis which was ameliorated by sGC stimulation. Our model may be a novel mouse model of gastrointestinal fibrosis in C57BL/6J mice corresponding to human systemic sclerosis.

Abbreviations

αSMA: alpha smooth muscles actin; BLM: bleomycin; cDNA: complementary deoxyribonucleic acid; cGMP: cyclic guanosine monophosphate; CIPO: chronic intestinal pseudo obstruction; COL1A1: collagen 1a1; COL3A1: collagen 3a1; CTGF: collagen tissue growth factor; DMSO: dimethyl sulfoxide; DSS: dextran sodium sulfate; GAPDH: glyceraldehyde-3-phosphate dehydrogenase; IL-1β: interleukin-1β; IL-6: interleukin-6; ITR%: intestinal transit rates; LPS: lipopolysaccharide; MT: Masson's trichrome; NS: normal saline; PAH: pulmonary artery hypertension; PKG: protein kinase G; TGFβ: transforming growth factor β; TNFα: tumor necrosis factor α; Scl-GvHD: sclerodermatous chronic graft-versus-host-disease; sGC: soluble guanylate cyclase; SSc: Systemic sclerosis.

Declarations

Ethics approval and consent to participate

This study contains no human data. All animal protocols were received prior to the approval of the institutional review board, and all procedures were performed in accordance with the recommendations of the Institutional Animal Care Committee of Kobe University.

Consent for publication

Not applicable.

Availability of data and materials

Not applicable.

Competing interests

The authors declare that they have no competing interests.

Funding

Not applicable.

Authors' contributions

YY and JS contributed to the study conception and design. YY, TO, HY, KA, SS and YU performed the experiments. YY, TO, AM, JS analyzed data and interpreted the data. YY drafted the manuscript, and OT, AM and JS revised it. All authors read and approved the final manuscript. JS takes the overall responsibility.

Acknowledgements:

The authors thank Shino Natsui for providing technical assistance.

Authors' information (optional)

Not applicable.

References

1. Ho YY, Lagares D, Tager AM, Kapoor M. Fibrosis-a lethal component of systemic sclerosis. Nat Rev Rheumatol. 2014;10:390–402.
2. Rogai V, Lories RJ, Guiducci S, Luyten FP. M Matucci Cerinic. Animal models in systemic sclerosis. Clin Exp Rheumatol. 2008; 26: 941–6.
3. Sarasadat H, Mohsen I, Hossein H, Gholamreza K. Effects of plant extracts and bioactive compounds on attenuation of bleomycin-induced pulmonary fibrosis. Biomed Pharmacother. 2018;107:1454–65.
4. Lee R, Reese C, Bonner M, Tourkina E, et al. Bleomycin delivery by osmotic minipump: similarity to human scleroderma interstitial lung disease. Am J Physiol Lung Cell Mol Physiol. 2014;306:736–48.
5. Isabel M, McFarlane MS, Bhamra A, Kreps S, Iqbal, et al. Gastrointestinal Manifestations of Systemic Sclerosis. Rheumatology. 2018;8:235. 10.4172/2161-1149.1000235.
6. Anton E. Nat Rev Gastroenterol Hepatol. 2016;13(8):461–72.
7. John B, Miller, Nisarg G, John C, Zsuzsanna M. Gastrointestinal Involvement in Systemic Sclerosis: An update. J Clin Rheumatol. 2018;24(6):328–37.
8. Takehiro T, Yoshihide A, Koji S, Takashi Y, Kouki N, Ryosuke S, et al. Epithelial Fli1 deficiency drives systemic autoimmunity and fibrosis: Possible roles in scleroderma. J Exp Med. 2017;214(4):1129–51.
9. Emma C, Derrett-Smith A, Dooley, et al. Endothelial injury in a transforming growth factor β-dependent mouse model of scleroderma induces pulmonary arterial hypertension. Arthritis Rheum. 2013;65:2928–39. DOI:10.1002/art.38078.
10. Peter S, Johannes Peter Stasch. Anti-fibrotic effect of solule guanylate cyclase stimulators and activators: A review of the preclinical evidence. Respir Med. 2017;122:1–9.
11. Clara D, Christian B, Alfiya D, Alina S, et al. Stimulators of soluble guanylate cyclase (sGC) inhibit experimental skin fibrosis of different aetiologies. Ann Rheum Dis. 2015;74(8):1621–5.

12. Harrison JH Jr, Lazo JS. High dose continuous infusion of bleomycin in mice: a new model for drug-induced pulmonary fibrosis. J Pharmacol Exp Ther. 1987;243:1185–94. PMID: 2447265.
13. Yoshinori A, Masami K, Yuki Y, et al. Role of platelet-derived growth factor/platelet-derived growth factor receptor axis in the trafficking of circulating fibrocytes in pulmonary fibrosis. Am J Respir Cell Mol Biol. 2014;51(6):793–801.
14. Tetsuji I, et al. Ameliorative effects of mosapride or rikkunshi-to on the suppression of gastrointestinal motility by pirfenidone in rats. Japanese Pharmacology Therapeutics. 2012;40:405–11. abstract (lifescience.co.jp).
15. Erdal Y, Nesrin G. Esophagectomy in scleroderma: report of a case. Case Rep Gastroenterol. 2008;2:449–504. DOI:10.1159/000161565.
16. Yuanyuan X, Wenjun L, et al. The effect of phycocyanin on bleomycin-induced pulmonary fibrosis and intestinal microbiota in C57BL/6 mice. Appl Microbiol Biotechnol. 2019;103:8559–69.
17. Hunerwadel A, Fagagnini S, et al. Severity of local inflammation does not impact development of fibrosis in mouse models of intestinal fibrosis. Sci Rep. 2018;8:15182. DOI:10.1038/s41598-018-33452-5.
18. Mishra A, et al. Esophageal remodeling develops as a consequence of tissue specific IL-5-induced eosinophilia. Gastroenterology. 2008;134:204–14.
19. Jamil S, Abul S. Chronic Intestinal Pseudo-Obstruction in Systemic Sclerosis: An Uncommon Presentation. Case Rep Gastroenterol. 2018;12(2):373–8.
20. Rieder F, Kessler S, et al. Animal models of intestinal fibrosis: new tools for the understanding of pathogenesis and therapy of human disease. Am J Physiol Gastrointest Liver Physiol. 2012;303:786–801.
21. Christopher L, Panja M, Boehm, Yasemin K, Eslam S, et al. Combined Activation of Guanylate Cyclase and Cyclic AMP in Lung Fibroblasts as a Novel Therapeutic Concept for Lung Fibrosis. Biomed Research International. 2019; 1345402. https://doi.org/10.1155/2019/1345402.
22. McCormick LL, Zhang Y, Tootell E, Gilliam AC. Anti-TGF-beta treatment prevents skin and lung fibrosis in murine sclerodermatous graft-versus-host disease: a model for human scleroderma. J Immunol. 1999;163:5693–9. PMID: 10553100.
23. Kevin K, Kim, Dean S, Harold A, Chapman. TGF-β1 Signaling and Tissue Fibrosis. Cold Spring Harb Perspect Biol. 2018;10(4):a022293.
24. Chu AJ, Prasad JK. Up-regulation by human recombinant transforming growth factor beta-1 of collagen production in cultured dermal fibroblasts is mediated by the inhibition of nitric oxide signaling. J Am Coll Surg. 1999;188(3):271–80.
25. Anna R, Hemnes, Ari Z, et al. PDE5A inhibition attenuates bleomycin-induced pulmonary fibrosis and pulmonary hypertension through inhibition of ROS generation and RhoA/Rho kinase activation. Am J Physiol Lung Mol Physiol. 2008;294:24–33.
26. Marc H, Gerry Coghlan J, et al. Riociguat for the treatment of pulmonary arterial hypertension associated with connective tissue disease: results from PATENT-1 and PATENT-2. Ann Rheum Dis.

2017;76(2):422–6.

27. Oliver D, Janet P, Chris D, et al. RISE-SSc: Riociguat in diffuse cutaneous systemic sclerosis. Respir Med. 2017;122(Suppl 1):14–7.
28. Vivek N, Cathie S, Erica B, Pei-Suen T, et al. A multicenter randomized, double-blind, placebo-controlled pilot study to assess the efficacy and safety of riociguat in systemic sclerosis-associated digital ulcers. Arthritis Res Ther. 2019;21(1):202.

Figures

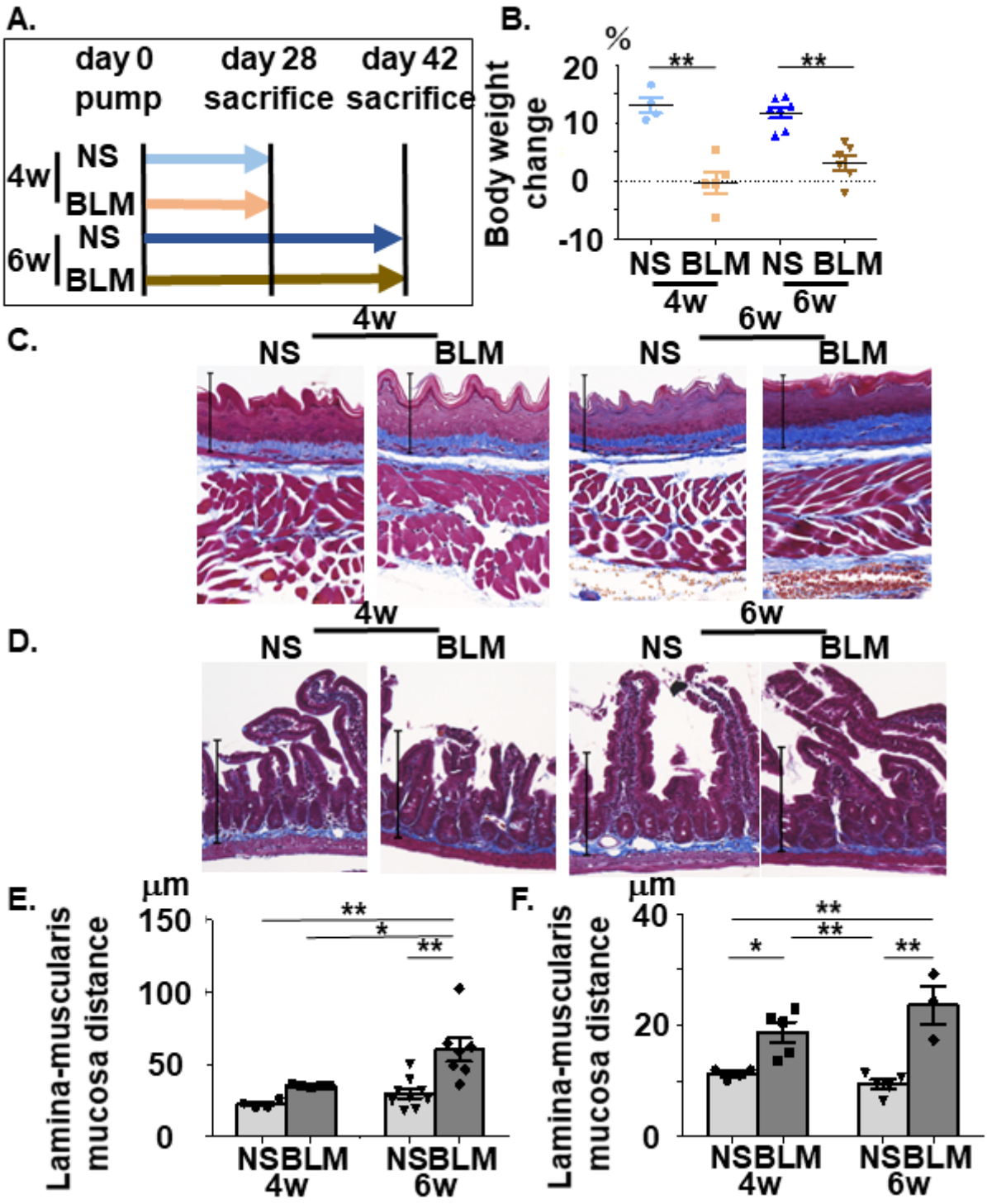

Figure 1

Bleomycin (BLM) caused esophageal and intestinal fibrosis. A, Schematic representation of the experimental protocol. Osmotic pumps containing 200 µL of BLM (125 mg/kg) or NS were implanted subcutaneously onto the backs of C57BL/6 mice on day 0. The pumps delivered their contents at a rate of 1.0 µg/h for 7 days. These mice were then sacrificed on day 28 (4 w) or day 42 (6 w). B, Body weight change from day 0 to day 28 or day 42 in C57BL/6 mice. The body weight change was calculated as [(body weight on day 28 or day 42) - (body weight on day 0)] ×(body weight on day 0)-1×100(%). Each

dot indicates the body weight change of an individual mouse. C, D, Representative images of esophageal (C) and intestinal (D) sections stained with Masson's trichrome (MT) at 40× magnification. (C: The straight line represents 100 μm. D: The straight line represents 200 μm). E, F, The thickness (lamina–muscularis mucosa distance) of esophageal (E) and intestinal (F) fibrotic tissue stained with MT (n = 5–7 mice per group). Bars represent mean ± SEM. *P < 0.05, **P < 0.01; One way ANOVA, Tukey's multiple comparison test. NS: normal saline, BLM: bleomycin.

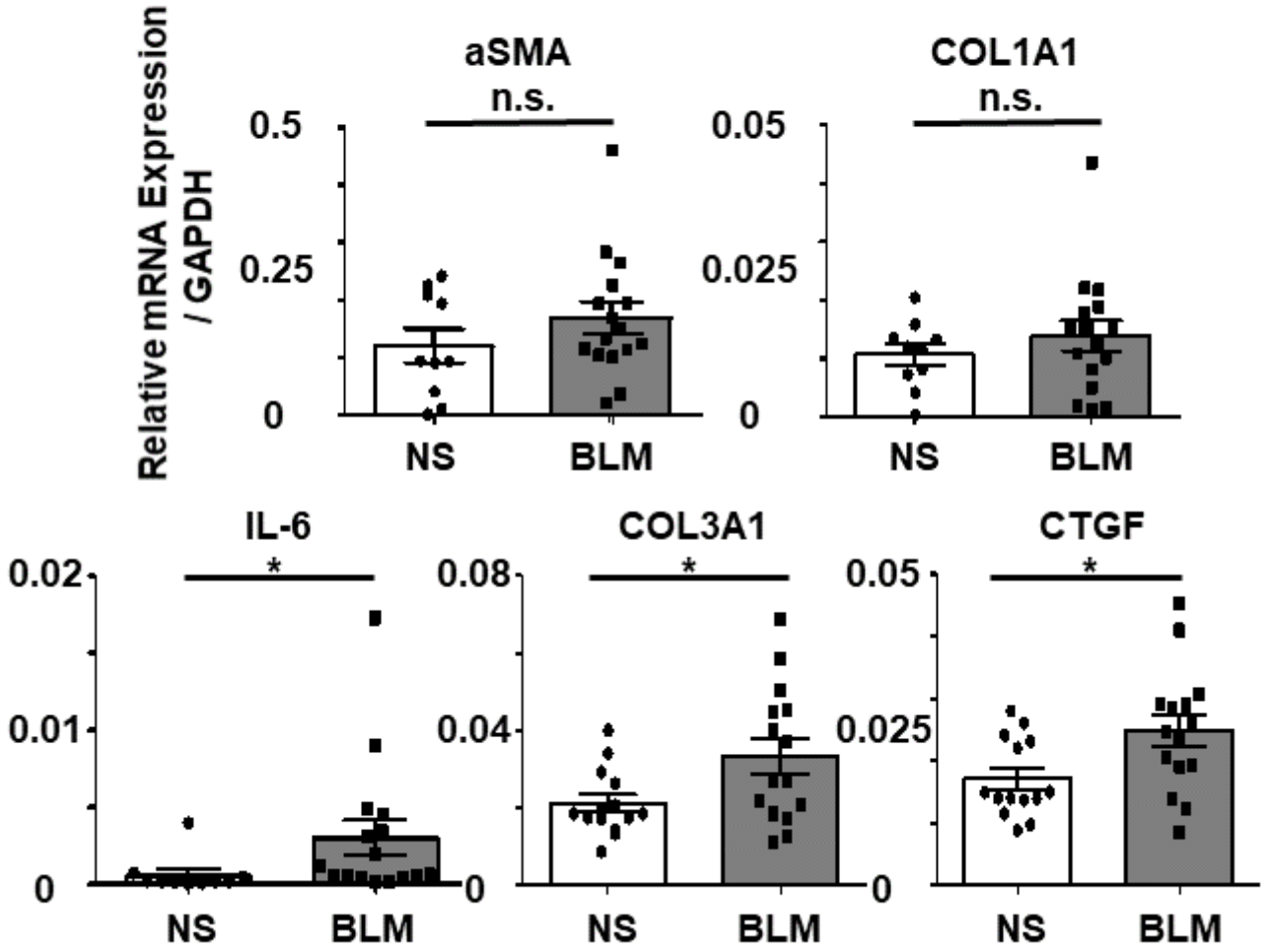

Figure 2

BLM induced fibrotic gene expression in the murine esophagus. Osmotic pumps containing 200 μL of BLM (125 mg/kg) or NS were implanted subcutaneously onto the backs of C57BL/6 mice on day 0. These mice were sacrificed on day 42 (6 w). Real-time PCR determined gene expression levels in the esophagus from BLM- or NS-treated mice. αSMA, COL1A1, IL-6, COL3A1, CTGF. Bars represent mean ± SEM. *P < 0.05, n. s. = not significant; unpaired t test with Welch's correction (n = 14–15 mice per group). αSMA: alpha smooth muscles actin, COL1A1: collagen 1a1, IL-6: interleukin-6, COL3A1: collagen 3a1, CTGF: connective tissue growth factor.

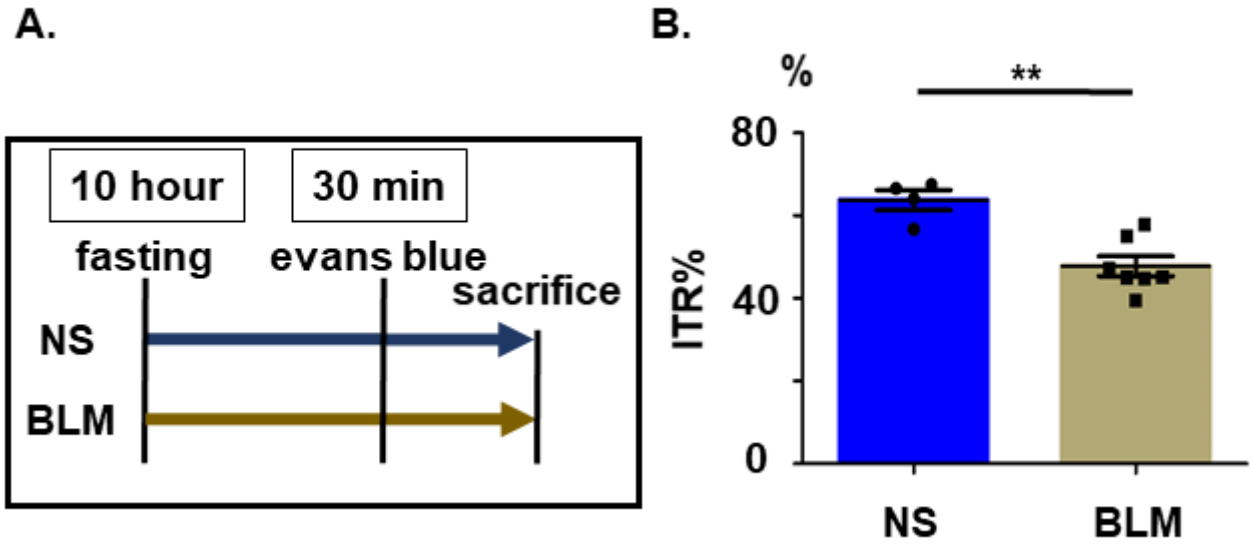

Figure 3

BLM reduced the peristaltic distance of the upper gastrointestinal tract in mice. A, Schematic representation of the experimental protocol. Osmotic pumps containing 200 µL of BLM (125 mg/kg) or NS were implanted subcutaneously onto the backs of C57BL/6 mice on day 0. On day 42 (6 w), the mice were fasted overnight but given free access to water. Next day the mice were orally administered 200 µL of Evans blue solution (5% w/v in NS), and sacrificed 30 min later. The rate of gastrointestinal transit was calculated by dividing the distance of the Evans blue migration by the total length of the small intestine. B, ITR% in BLM- or NS- treated C57BL/6 mice (n = 5–7 mice per group). Bars represent mean ± SEM. **P < 0.01; Unpaired t test with Welch's correction (n = 14–15 mice per group).

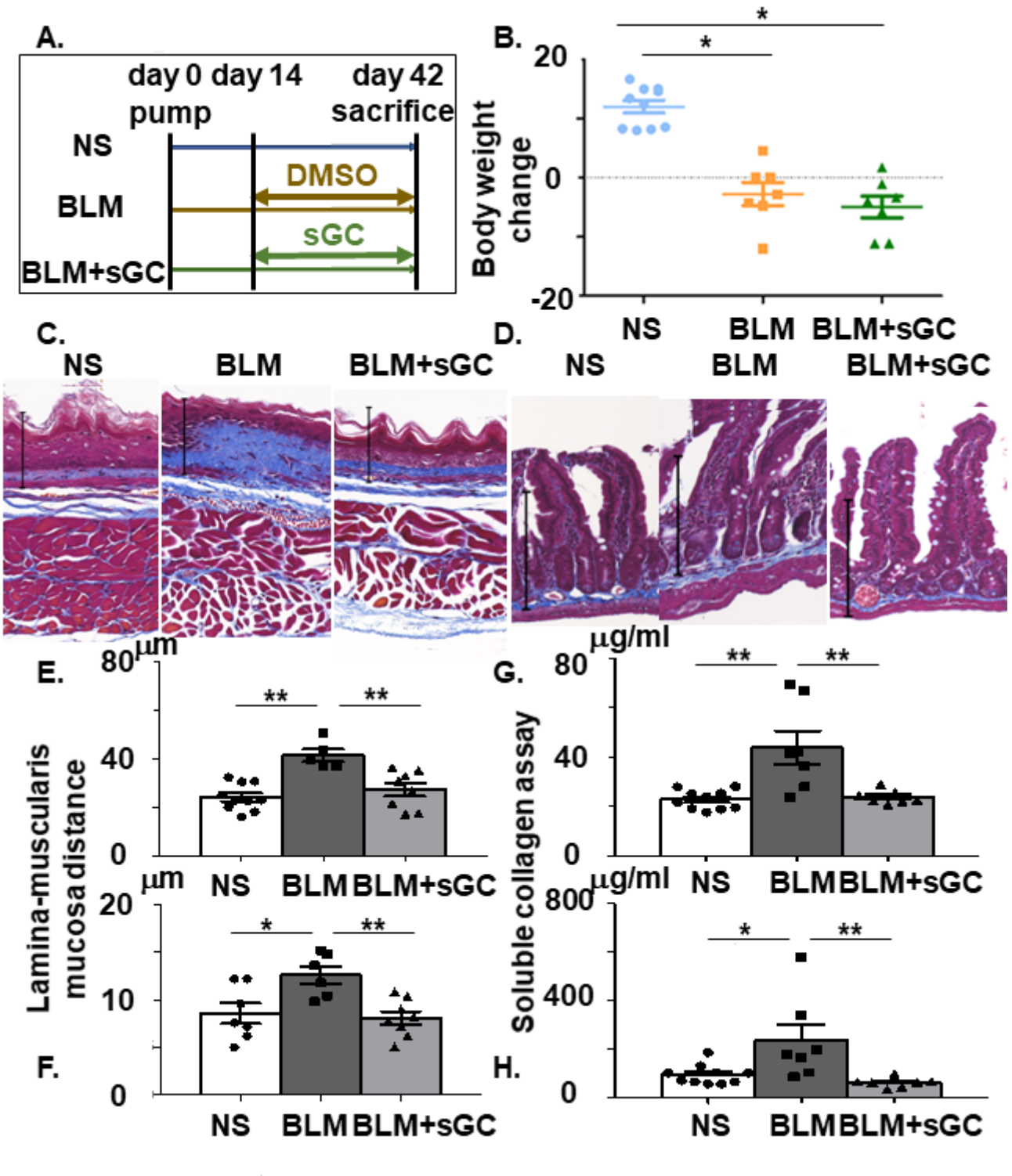

Figure 4

Treatment with a soluble guanylate cyclase (SGC) agonist improved esophageal and intestinal fibrosis. A, Schematic representation of the experimental protocol. Osmotic pumps containing 200 µL of BLM (125 mg/kg) or NS were implanted on day 0. Pumps were removed on day 7. Mice were then treated with an oral sGC agonist, BAY 63-2521, (10 mg/kg) (BLM+sGC group) or DMSO (BLM group) from day 14 to day 42, then sacrificed on day 42 (6 w). B, Body weight change from day 0 to day 42 in C57BL/6 mice. The body weight change was calculated as [(body weight on day 42) - (body weight on day 0)] ×(body weight

on day 0)-1×100 (%). (n = 6–10 mice per group). C, D, Representative histology of esophagus (C) and intestine (D) stained with MT at 40× magnification. (C: The straight line represents 100 μm. D: The straight line represents 200 μm). E, F, The thickness (lamina–muscularis mucosa distance) of fibrosis in esophagus (E) and intestine (F) fibrotic tissues stained with MT (n = 6–10 mice per group). G, H, Soluble collagen production in esophagus (G) and intestine (H) in NS-, BLM-, and BLM-sGC-agonist-treated mice (n = 6–10 mice per group). Bars represent mean ± SEM. *P < 0.05, **P < 0.01; One way ANOVA, Tukey's multiple comparison test. sGC: soluble guanylate cyclase

Supplementary Files

This is a list of supplementary files associated with this preprint. Click to download.

- Additionalfile1.pptx